

## Lifetime Measurements of Spherical and Deformed States in $1f_{7/2}$ Nuclei

N.H. Medina,<sup>1</sup> F. Brandolini,<sup>2</sup> S.M. Lenzi,<sup>2</sup> N. Mărginean,<sup>3</sup>  
R.V. Ribas,<sup>1</sup> C.A. Ur,<sup>2</sup> D. Bazzacco,<sup>2</sup> S. Lunardi,<sup>2</sup> R. Menegazzo,<sup>2</sup>  
P. Pavan,<sup>2</sup> C. Rossi-Alvarez,<sup>2</sup> A. Algora-Pineda,<sup>3</sup> G. de Angelis,<sup>3</sup>  
M. De Poli,<sup>3</sup> E. Farnea,<sup>3</sup> A. Gadea,<sup>3</sup> T. Martinez,<sup>3</sup> D.R. Napoli,<sup>3</sup>  
S. Hankonen,<sup>4</sup> D. Bucurescu,<sup>5</sup> M. Ionescu-Bujor,<sup>5</sup> A. Iordachescu,<sup>5</sup>  
J.A. Cameron,<sup>6</sup> S. Kasemann,<sup>7</sup> I. Schneider,<sup>7</sup> J.M. Espino,<sup>8</sup>  
J. Sanchez-Solano<sup>9</sup> and A. Poves<sup>9</sup>

<sup>1</sup> Instituto de Física, Universidade de São Paulo, São Paulo, Brazil

<sup>2</sup> Dipartimento di Fisica dell'Università and INFN, Sez. di Padova, Padova, Italy

<sup>3</sup> Laboratori Nazionali di Legnaro, Legnaro, Italy

<sup>4</sup> Department of Physics, Jyväskylä, Finland

<sup>5</sup> National Institute of Physics and Nuclear Engineering, Bucharest, Romania

<sup>6</sup> McMaster University, Ontario, Canada

<sup>7</sup> Institut für Kernphysik der Universität zu Köln, Köln, Germany

<sup>8</sup> Departamento de Física, Universidad de Sevilla, Sevilla, Spain

<sup>9</sup> Dept. de Física Teórica, Universidad Autónoma de Madrid, Madrid, Spain

*Received 18 October 2001*

**Abstract.** Lifetimes have been determined using the Doppler Shift Attenuation Method in the  $N \approx Z$  nuclei  $^{46}\text{V}$  and  $^{48}\text{V}$  nuclei, populated with the reaction  $^{28}\text{Si}$  on  $^{24}\text{Mg}$  at 115 MeV and  $^{24}\text{Mg}$  on  $^{28}\text{Si}$  at 100 MeV using Au and Pb backed targets. The coexistence of spherical and deformed states in the middle of the  $1f_{7/2}$  shell is discussed. The  $B(E2)$  and  $B(M1)$  reduced rates agree very well with large scale shell model predictions.

*Keywords:* nuclear reactions  $^{28}\text{Si} + ^{24}\text{Mg}$  at 115 MeV and  $^{24}\text{Mg} + ^{28}\text{Si}$  at 100 MeV, measured  $E_\gamma$  and  $\gamma\text{-}\gamma$  coincidence, DSAM,  $^{46,48}\text{V}$  deduced high-spin levels,  $J, \pi, B(E2), B(M1)$

*PACS:* 21.10.Tg, 23.20.-g, 23.20.Lv, 27.40.+z

## 1. Introduction

In recent years a great deal of spectroscopic information has been collected at the Legnaro National Laboratories (LNL) for nuclei near the middle of the  $1f_{7/2}$  shell, in particular for  $^{48,49,50}\text{Cr}$  and  $^{47}\text{V}$  [1–5]. Many rotational-like bands have been found. Prolate or somewhat triaxial deformation is built at low spin, which evolves toward a spherical shape approaching the band termination, i.e. the maximum spin available in the configuration space. Since the deduced  $B(E2)$  reduced rates can give information about rotational collectivity and  $B(M1)$  reduced rates are indicators of single particle features, lifetime of excited states have been determined with the Doppler Shift Attenuation Method (DSAM). Large Scale Shell Model (LSSM) calculations in the full fp configuration space [7] reproduce very well the excitation energies of the observed natural parity levels and their transition probabilities, while the unnatural parity levels are reasonably well reproduced by extending the configuration space to include a  $d_{3/2}$ -hole [8].

This contribution will present recent results on the  $N = Z$  odd–odd nucleus  $^{46}\text{V}$  [9] and the odd–odd  $N = Z + 2$   $^{48}\text{V}$  nucleus [10]. Odd–odd nuclei may provide a stringent test for LSSM, due to sensitivity for the proton–neutron residual interaction. The  $^{46}\text{V}$  nucleus has been studied recently with great interest owing to its special characteristics [11–14]. As shown in the level scheme of Fig. 1, coexistence of natural parity  $T = 1$  states with  $T = 0$  and unnatural parity states occurs at low excitation energy, allowing the verification of isospin selection rules and isospin mixing. In Ref. [11] a detailed level scheme was obtained and compared with LSSM predictions. The  $^{48}\text{V}$  nucleus was shown to provide more experimental information owing to its strong population in fusion reactions. Previous data on  $^{48}\text{V}$  can be found in Refs [15, 16].

## 2. Experimental Procedure and Results

The study of the  $^{46}\text{V}$  and  $^{48}\text{V}$  nuclei was performed using thin (selfsupporting) and thick (backed) targets. In the first experiment the fusion reaction  $^{24}\text{Mg}$  on  $^{28}\text{Si}$  at 100 MeV has been used with a  $0.4 \text{ mg/cm}^2$   $^{28}\text{Si}$  selfsupporting target. Gamma rays were detected with the GASP array, comprising 40 Compton-suppressed HPGe detectors and an 80-element BGO ball which acts as a gamma-ray multiplicity filter [17]. Light charged particles were detected with the ISIS array, consisting of 40  $(\Delta E, E)$  Si telescopes [18]. In the second experiment the inverse reaction  $^{28}\text{Si}$  on  $^{24}\text{Mg}$  at 115 MeV bombarding energy has been employed, using  $0.8 \text{ mg/cm}^2$  targets backed with  $15 \text{ mg/cm}^2$  of either Au or Pb. In order to increase the  $\gamma$ – $\gamma$  counting rate the ISIS array was not used in this experiment. The energy in the center of mass frame was the same in the two measurements. In both measurements, events were stored when at least two Ge detectors and two elements of the multiplicity filter fired in coincidence. Energy and efficiency calibrations were performed with sources of  $^{152}\text{Eu}$  and  $^{56}\text{Co}$  and  $^{60}\text{Co}$ , as well as with known internal narrow lines.

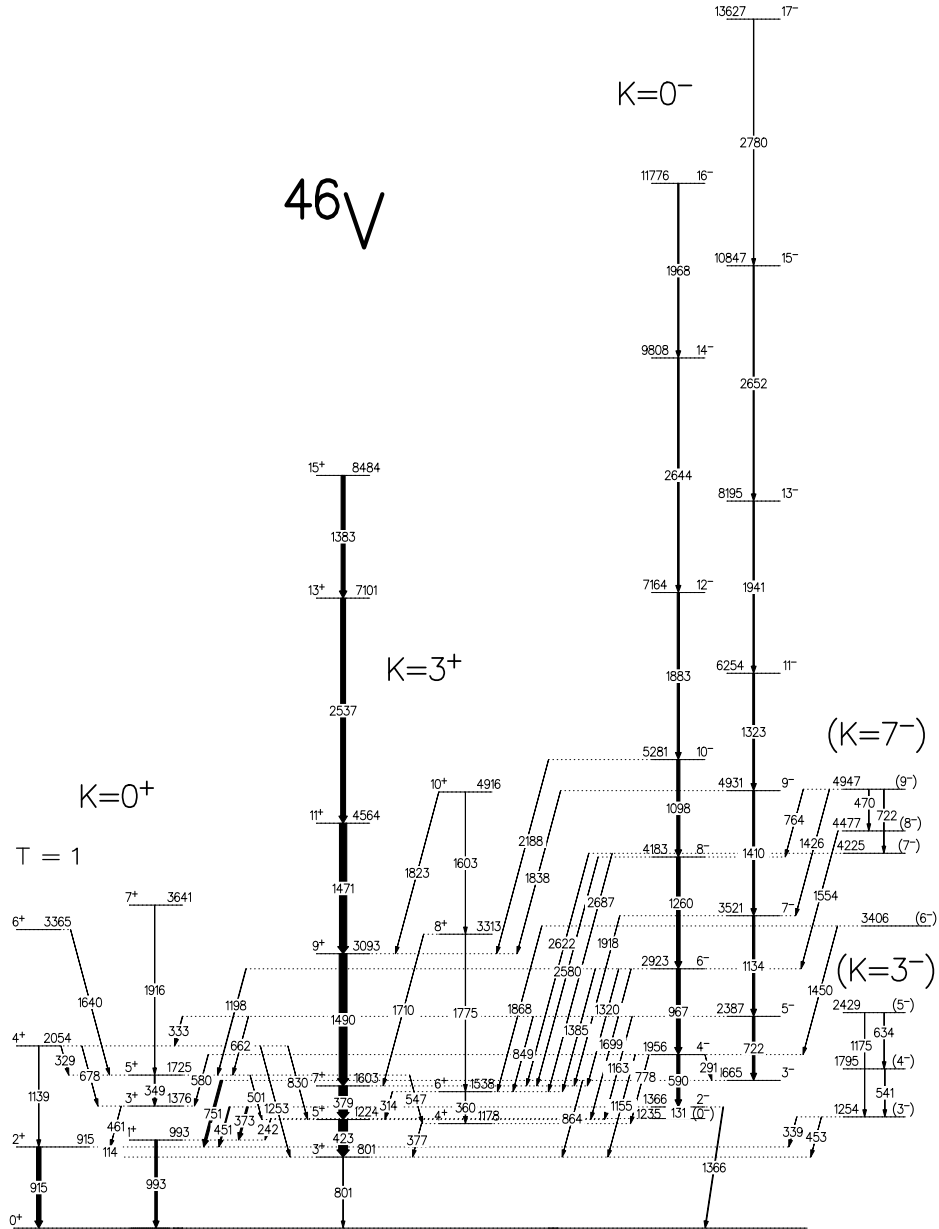
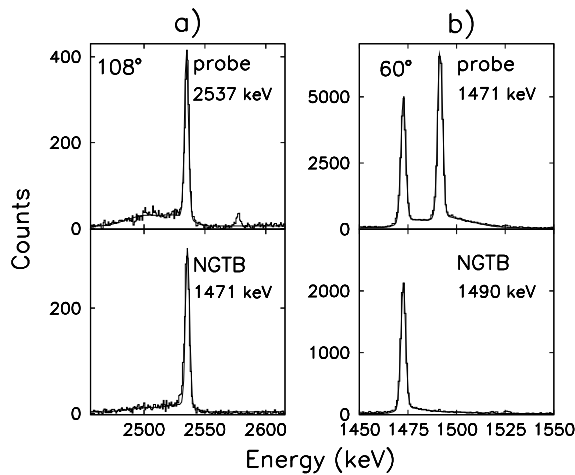


Fig. 1. Level scheme of the  $^{46}\text{V}$  nucleus

### 2.1. Lifetime measurements

For the lifetime measurements, data from the thick target measurement were sorted into seven  $\gamma$ - $\gamma$  matrices having on the first axis the detectors in rings at  $34^\circ$ ,  $60^\circ$ ,  $72^\circ$ ,  $90^\circ$ ,  $108^\circ$ ,  $120^\circ$ ,  $146^\circ$  and on the second axis any of the other 39 detectors. More details of the analysis procedure are reported in Ref. [3]. The program LINE-SHAPE [19] was modified in order to allow the Narrow Gate on Transition Below (NGTB) procedure [6], which is free from systematic errors related with sidefeeding uncertainties. As an example, the lineshape of two transitions with the method NGTB is shown in Fig. 2. With an upper coincident transition as a probe, the comparison of its full lineshape (upper part of the figure) with the partly suppressed lineshape (lower part), obtained with a narrow gate on the transition to be studied, provides its lifetime. The Northcliffe-Schilling stopping power [20], corrected for atomic shell effects [21], was used. The measurement with lead as backing material was lower in statistics by more than a factor of two with respect to that using Au, but it was important in order to extend the lifetime measurement to longer lived states.



**Fig. 2.** NGTB lifetime analysis in  $^{46}\text{V}$ . a) 1471 keV  $11^+ \rightarrow 9^+$  transition. b) 1490 keV  $9^+ \rightarrow 7^+$  transition. A gold backing was employed.

The lifetime of 25 states have been determined in  $^{48}\text{V}$ , and 14 states in  $^{46}\text{V}$ ; most of them were obtained with the NGTB procedure, which is, in principle, superior compared with the standard analysis because it avoids the systematic errors caused by the complex decay pattern.

### 2.2. The $^{46}\text{V}$ nucleus

The level scheme of the  $^{46}\text{V}$  nucleus is organized in rotational bands of definite K values, shown in Fig. 1. The  $K = 0^+$  and  $K = 3^+$  bands are expected to originate from the parallel and antiparallel coupling of the Nilsson orbitals  $[321]3/2^-$  occupied

by the odd nucleons, respectively. The antiparallel coupling gives rise to the  $K = 0^+$  ground state band, shown in the left of Fig. 1, where the even spin levels have  $T = 1$ . The most intense positive parity band, based on the yrast  $3^+$  level and terminating at the  $15^+$  level, can be described as the  $K = 3^+$  sequence with favored signature. A third band, indicated in Fig. 1 with  $K = 0^-$  is described as due to the excitation of a  $d_{3/2}$  hole. The  $K = 3^-$  and  $K = 0^-$  bands, are expected to originate from the parallel and antiparallel coupling of the orbitals  $[202]3/2^+$  and  $[321]3/2^-$ . A candidate for the  $0^-$  head of the former band has been observed, and a candidate for the head of the  $K = 3^-$  band, due to the parallel coupling, is observed at 1254 keV, as well as the next two levels, already observed in Refs [11, 14]. A very weak band, based on a known level at 4225 keV [11], is now classified as  $K = (7^-)$ . This band is predicted in the Nilsson scheme, as due to the excitation of a nucleon from the  $[202]3/2^+$  orbital to the empty orbital  $[321]5/2^-$ , with a parallel coupling of the 4 unpaired nucleons. Several weak E1 branches have been observed to connect the  $K = 0^-$  band to positive parity levels.

Lifetimes for eleven levels of the  $K = 0^-$  band could be determined, leading to  $B(E2)$  values well reproduced by LSSM calculations, as shown in Fig. 3. LSSM calculations were performed with the code ANTOINE, using the KB3 residual interaction [7]. Such calculations compared with experimental data have been already reported in Ref. [11]. The lifetimes of the  $4^-$  and  $5^-$  states are too long for DSAM analysis. The regular pattern of the low part of the  $K = 0^-$  band suggests a rotor-like behaviour down to  $I = 2^-$ . The strong backbending of the  $\alpha = 0$  signature band at  $I^\pi = 10^-$  is accompanied by a drastic decrease of the  $B(E2)$  value. Both of them are well reproduced by LSSM. The  $\Delta I = 1$  branches were not observed in the negative parity band, except for the  $4^- \rightarrow 3^-$  transition, but with only 1.0(3)%.

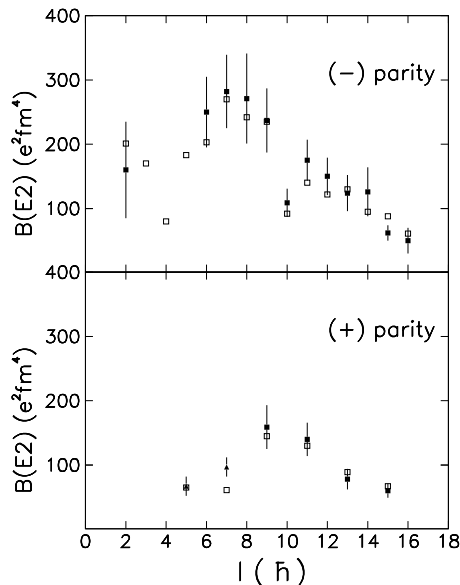


**Fig. 3.** Experimental  $B(E2)$  reduced transition rates in  $^{46}\text{V}$ , compared with LSSM prediction (empty squares). Experimental values are taken from the present work (full squares) except for the values indicated as full triangles.

According to the isospin selection rule [22],  $\Delta T = 0$  M1 transitions are predicted to be very hindered, so that this branch is likely mainly E2.

In the  $K = 3^+$  band, only the  $B(E2)$  values for transitions between levels of the favored signature could be determined and were found to be in good agreement with LSSM calculations, as shown in Fig. 3. A deformation parameter  $\beta \approx 0.22$  is deduced from the reduced rates of  $11^+ \rightarrow 9^+$  and  $9^+ \rightarrow 7^+$  transitions. The LSSM calculations are in good agreement with the experimental data also for levels of the  $K = 0^+$  band.

### 2.3. The $^{48}\text{V}$ nucleus

The level scheme of the nucleus  $^{48}\text{V}$  is shown in Fig. 4. The level scheme has been extended to high spin states mainly with the thin target measurement data, both from  $\gamma\text{-}\gamma\text{-}\gamma$  coincidence cube and from  $\gamma\text{-}\gamma$  matrices in coincidence with 3 protons detected with the ISIS array. Thick target measurement was used mainly for lifetime measurements, which also provided parity assignment for new high spin levels. The observed levels are grouped in 5 bands, classified with  $K = 4^+, 1^+, 4^-, 1^-$  and  $8^-$ , respectively. It has to be stressed the similarity with  $^{46}\text{V}$  where also 5 bands of similar nature have been observed. The main difference between  $^{46}\text{V}$  and  $^{48}\text{V}$  is that in  $^{46}\text{V}$  both unpaired neutron and protons are in the same orbital  $[321]3/2^-$ , while in  $^{48}\text{V}$  the last neutron is in the  $[312]5/2^-$  one. Therefore, while in  $^{48}\text{V}$  two positive parity bands with  $K = 4^+$  and  $1^+$  originate, in  $^{46}\text{V}$  they have  $K = 3^+$  and  $0^+$ . Similarly, the excitation of a proton from the  $d_{3/2}$  orbital  $[202]3/2^+$  to the next available orbital give rise to negative parity bands classified as  $K = 4^-$  and  $1^-$  for the  $^{48}\text{V}$ , while in  $^{46}\text{V}$  they are classified as  $K = 3^-$  and  $0^-$  bands. Finally, the excitation from the  $[202]3/2^+$  orbital to the first empty orbital, followed by the parallel coupling of the four unpaired nucleons, gives rise to the  $K = 7^-$  band in  $^{46}\text{V}$ , and a  $K = 8^-$  for  $^{48}\text{V}$  nuclei.

The level energy predictions performed with the LSSM for both positive yrast and yrare bands are in excellent agreement considering the complexity of the level scheme [10]. Calculations have been performed also for the negative parity states, allowing a hole in the  $2d_{3/2}$  orbital and taking a cut at three in the number of nucleons outside the  $1f_{7/2}$  orbital. In this case the agreement is rather good taking into account the truncation made. The staggering of the  $K = 1^-$  band is well reproduced. Nevertheless, the  $K = 8^-$  band is calculated about five hundred keV lower than measured, while the  $K = 4^-$  band is only about two hundred keV lower than measured.

An example of NGTB analysis for the positive parity yrast band is shown in Fig. 5. It has to be remarked the very pronounced lineshape of most of the observed transitions. The deduced  $B(M1)$  rate is very large for the  $15^+ \rightarrow 14^+$  transition and shows a staggering down to low spins, which is accompanied by a smooth behavior of the  $B(E2)$  values. Such staggering behavior is an effect related to the  $1f_{7/2}^n$  configuration. In Fig. 6 is shown the reduced transition rates for the yrast positive parity states in  $^{48}\text{V}$ , compared with theoretical predictions. The decrease



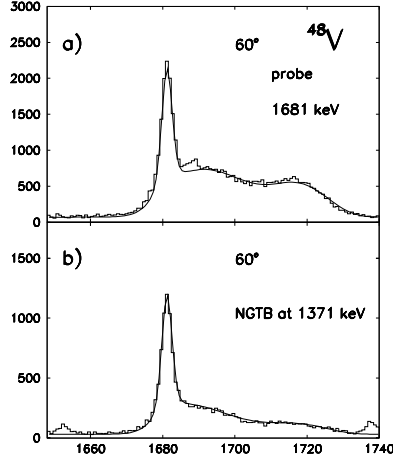


**Fig. 5.** NGTB lifetime analysis for the 1371 keV  $9^+ \rightarrow 7^+$  transition

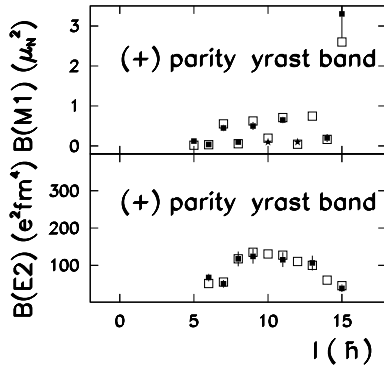


**Fig. 6.** Reduced transition rates for the yrast positive parity states in  $^{48}\text{V}$  (closed squares), compared with theoretical predictions (open squares). The full stars refer to values normalized to theoretical  $B(E2)$  predictions.

of the  $B(E2)$  for the high spin states indicates the reduction of the collectivity when approaching the band termination, as the levels become rather pure  $1f_{7/2}^n$  states. The  $B(M1)$  values show for the natural parity band a large staggering, when approaching the band termination, as they are particularly sensitive to single-particle features. The lifetime of the yrast  $10^+$ ,  $12^+$  and  $14^+$  states could not be measured due to the low statistics. The corresponding  $B(M1)$  values, marked with full stars in Fig. 6, were obtained by adopting the theoretical  $B(E2)$  values for the  $\Delta I = 2$  branches, with 50% error; it is a general feature that  $B(E2)$  values for yrast levels are well predicted by LSSM in the middle of the  $1f_{7/2}$  shell. From the lower states we extract a quadrupole deformation parameter  $\beta \simeq 0.21$ , under the assumption of a  $K = 4^+$  band. This value is much smaller than the one observed in  $^{48}\text{Cr}$  of  $\beta \simeq 0.28$  [3]. It may be that the nucleus actually has a larger  $\beta$ , but that triaxiality with a positive value of  $\gamma$ , as suggested for  $^{46}\text{V}$  [12], gives rise to a smaller  $B(E2)$  value.

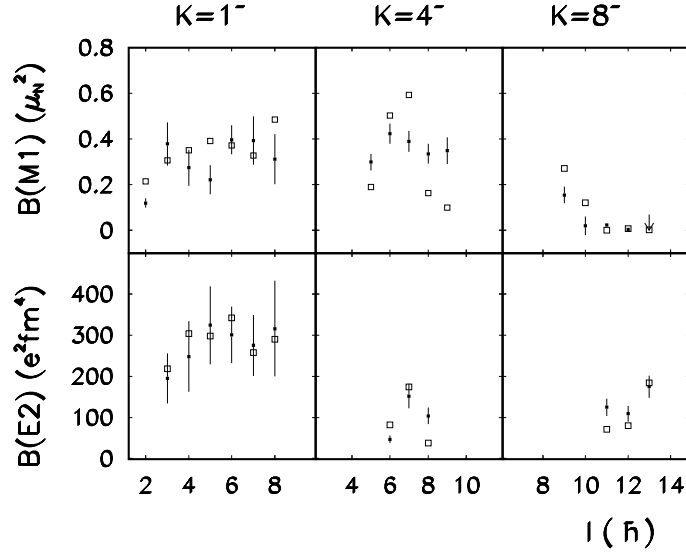


**Fig. 7.** Reduced transition rates for the negative parity states in  $^{48}\text{V}$ , compared with theoretical predictions. Closed squares are experimental values and open squares are the predictions.

Both negative parity bands  $K = 1^-$  and  $K = 4^-$  have little signature splitting pointing to small triaxiality. They can be described at low spin with a deformation parameter  $\beta \approx 0.26$ , giving rise to shape coexistence between bands of different parity, as observed for other nuclei in this region [5]. Some examples of reduced transition rates of the negative parity states are shown in Fig. 7 together with the predictions of the LSSM.

### 3. Conclusions

A considerable amount of information has been obtained for the structure of the  $^{46}\text{V}$  and  $^{48}\text{V}$  nuclei. The observed levels of both nuclei are grouped in 5 band structures. They are very well described in the frame of the Nilsson model.

In  $^{46}\text{V}$  the agreement with LSSM calculations for the positive parity levels is very good. Calculations for the negative parity states are satisfactory as they reproduce both the backbending and the drop in the  $B(E2)$  value at  $I^\pi = 10^-$  along the well deformed  $K = 0^-$  band. In  $^{48}\text{V}$  all observed spectroscopic quantities for positive parity states are in excellent agreement with LSSM calculations in the full fp shell. The agreement of the calculated reduced rates for negative parity levels is reasonably good, considering the space truncation, even if the levels are not well described around the region of bandcrossing between the  $K = 4^-$  and  $K = 8^-$  bands.

The B(E2) values in  $^{46,48}\text{V}$  show the building up of the collectivity at low spin in the bands of both natural and unnatural parities. The collectivity is reduced when approaching the band termination, as the levels become rather pure  $1f_{7/2}^n$  states. The B(M1) values for  $^{48}\text{V}$  show for the natural parity band a large staggering when approaching the band termination, as they are particularly sensitive to single-particle features.

## Acknowledgements

N.H.M. and R.V.R. would like to acknowledge financial support from the Brazilian agency CNPq (Conselho Nacional de Desenvolvimento Científico e Tecnológico) and INFN (Italy). A.P. and J.S.S. are supported by a DGES (Spain) grant PB96-53. The CCCFC (UAM) Spain provided part of the computer cycles employed in this work. A.G. was supported by the EC under contract ERBCHBGCT940713.

## References

1. S.M. Lenzi et al., *Z. Phys.* **A354** (1996) 117.
2. S.M. Lenzi et al., *Phys. Rev.* **C56** (1997) 1313.
3. F. Brandolini et al., *Nucl. Phys.* **A642** (1998) 387.
4. F. Brandolini et al., *Phys. Rev.* **C60** (1999) R041305.
5. F. Brandolini et al., *Nucl. Phys.* **A693** (2001) 517.
6. F. Brandolini and R.V. Ribas, *Nucl. Instr. Meth.* **A417** (1998) 150.
7. E. Caurier et al., *Phys. Rev. Lett.* **75** (1995) 2466.
8. A. Poves and J. Sanchez-Solano, *Phys. Rev.* **C58** (1998) 179.
9. F. Brandolini et al., *Phys. Rev.* **C** (in press).
10. F. Brandolini et al., *LNL Annual Report* (1999) and to be published.
11. S. Lenzi et al., *Phys. Rev.* **C60** (1999) 021303.
12. C.D. O'Leary et al., *Phys. Lett.* **B459** (1999) 73.
13. C. Friessner et al., *Phys. Rev.* **C60** (1999) 011304.
14. I. Schneider, *PhD Thesis*, Köln, 2001; P. v. Brentano et al., *Nucl. Phys.* **A682** (2001) ???.
15. T.W. Burrows, *Nuclear Data Sheets* **68** (1993) 1.
16. J. Cameron et al. *Phys. Rev.* **C49** (1994) 1347.
17. D. Bazzacco, *Proc. Int. Conf. on Nuclear Structure at High Angular Momentum*, Ottawa (1992) Report No. AECL 10613, Vol. 2, p. 376.
18. E. Farnea et al., *Nucl. Inst. Meth.* **A400** (1998) 87.
19. J.C. Wells and N. Johnson, Report No. ORNL-6689 (1991) 44.
20. L.C. Northcliffe and R.F. Schilling, *Nucl. Data Tables* **A7** (1970) 233.
21. S.H. Sie et al., *Nucl. Phys.* **A291** (1977) 11.
22. E.K. Warburton and J. Wesener, in *Isospin in Nuclear Physics*, ed. D.H. Wilkinson, North-Holland, Amsterdam, 1969.